Int. J. Solids Structures Vol. 19, No. 4, pp. 293–303, 1983
Printed in Great Britain.

0020-7683/83/040293-11$03.00/0
Pergamon Press Ltd.

INDENTATION OF A BEAM BY A RIGID CYLINDER

B. V. SANKAR and C. T. SUN
School of Aeronautics and Astronautics, Purdue University, West Lafayette, IN 47907, U.S.A.

(*Received* 14 *June* 1982)

Abstract—The problem of smooth indentation of a beam of finite length by a rigid, cylindrical indenter is studied. A simple method is developed to solve the two-dimensional problem of a beam subjected to an arbitrary but symmetrical loading on one side. The displacements are computed by superposing classical beam theory solution with the elasticity solution obtained through the use of finite Fourier transforms. The above method in conjunction with a point matching technique is used to solve the indentation problem. For small contact lengths, the contact stress distribution is assumed to be elliptical and the problem is solved in a more direct way. Values of overall deflection, indentation and contact lengths are computed and plotted as a function of total load.

NOTATION

c	semi contact length
$c_1 \ldots c_4, d_1 \ldots d_4$	elasticity solution constants
C	compliance
C^*	beam theory compliance
h	beam thickness
i	square root of -1
L	half length of beam
n	transform variable
P	total load
$p(x)$	load distribution
q_j	magnitude of jth pressure distribution
R	radius of indenter
s	slope of the deflection curve at the supports (calculated from beam theory)
u	horizontal displacement
v	vertical displacement
w_{jk}	vertical displacement of jth point due to kth load distribution of unit magnitude
x, y	horizontal and vertical coordinate axes
α	indentation
λ, μ	Lamé constants of beam material
κ	$(\lambda+3\mu)/(\lambda+\mu)$ for plane strain$(5\lambda+6\mu)/(3\lambda+2\mu)$ for plane stress
ξ	transform variable $(= n\pi/L)$
σ_{yy}	normal stress
τ_{xy}	shear stress

1. INTRODUCTION

The problem of indentation of a beam of finite length by a smooth cylindrical indenter is of great practical and analytical interest because the results deviate considerably from the Hertzian Solution for half-space due to bending effects. Keer and Miller[1] approached the above problem by superposition of an infinite layer solution with a pure bending beam theory solution. They calculated contact stresses and overall beam compliances for various ratios of contact area to layer thickness. Their method involves solving an integral equation for an auxiliary function and then using the same for calculating desired field quantities.

In this paper a simple method is used to solve the plane problem of a beam subjected to an arbitrary but symmetric normal loading on one side. The load is considered as the sum of an uniformly distributed load (U.D.L.) and a variable part of zero average value. The displacements due to the U.D.L. are obtained from the classical beam theory. The displacements due to the variable part are computed by solving the plane elasticity equations using finite Fourier transforms. The problem of indentation is solved by a point matching technique similar to that used by Conway[2]. A second method which consists of assuming the nature of stress distribution under the indenter is also developed for small contact areas.

The contact stresses and beam compliances agree well with[1]. For the case of beams,

indentation is defined as the difference in the vetical displacement of the indenter and that of the corresponding point on the bottom surface of the beam. The load-indentation relation is also obtained. This type of indentation law is of considerable interest in impact problems [3].

2. AUXILIARY PROBLEM

The problem considered in this section is that of finding the v (vertical)-displacements of a beam subjected to an arbitrary symmetrical loading $p(x)$ over a length 2c on the top surface of the beam (Fig. 1). The length of the beam is $2L$, thickness is h and the width is taken as unity.

The load $p(x)$ can be expressed in the form of a complex Fourier series in the interval $-L$ to $+L$. Thus,

$$p(x) = \frac{P}{2L} + \sum_{\substack{n=-\infty \\ n\neq 0}}^{\infty} a_n \, e^{in\pi x/L} \tag{1}$$

where

$$P = \int_{-c}^{+c} p(x)\,dx$$

$$a_n = \frac{1}{2L}\int_{-L}^{+L} p(x)\, e^{-i\xi x}\,dx \tag{2}$$

and

$$\xi = n\pi/L.$$

Actually $p(x)$ may be considered as the sum of two types of loadings, namely, a uniformly distributed load (U.D.L.) of intensity $P/2L$ and a varying part whose average value is equal to zero, i.e.

$$p(x) = P/2L + p_1(x). \tag{3}$$

The deflection of the beam due to the U.D.L. is obtained from the classical beam theory. The displacements due to $p_1(x)$ is obtained by solving the plane elasticity equations using finite Fourier transforms.

The superposition of the beam solution with the 2-D solution needs some justification. The problem of our interest is indentation of beams in which the contact length $2c$ will be very small compared to the beam length $2L$. Indentation is a local effect which will be influenced more by the load $p_1(x)$ rather than the U.D.L. Moreover, we can assume that the differences between beam solution and elasticity solution for vertical displacements will be negligible for the case of U.D.L.

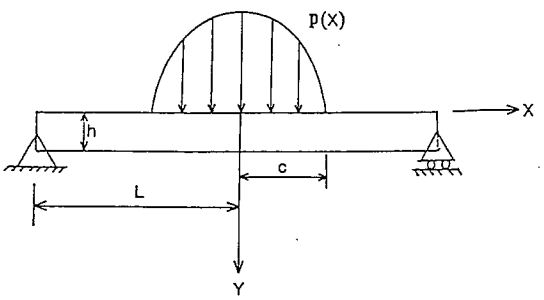

Fig. 1. Beam subjected to an arbitrary, symmetrical loading.

We define the finite Fourier transform of a function $f(x)$ as

$$\bar{f}(n) = \frac{1}{2L}\int_{-L}^{+L} f(x)\, e^{-in\pi x/L}\, dx.$$

Then the inverse transform will be

$$f(x) = f_0 + \sum_{\substack{n=-\infty \\ n\neq 0}}^{+\infty} \bar{f}(n)\, e^{in\pi x/L} \tag{4}$$

where f_0 is the average value of the function over the interval $-L$ to $+L$. From eqns (1–3), we have

$$\begin{aligned} \bar{p}_1(n) &= a_n; \quad n \neq 0 \\ &= 0; \quad n = 0. \end{aligned} \tag{5}$$

We now proceed to solve the two-dimensional problem of a beam subjected to the normal load $p_1(x)$ on the surface $y = 0$. The appropriate Navier's equations are:

$$\begin{aligned} (\kappa+1)u_{,xx} + (\kappa-1)u_{,yy} + 2v_{,xy} &= 0 \\ (\kappa-1)v_{,xx} + (\kappa+1)v_{,yy} + 2u_{,xy} &= 0. \end{aligned} \tag{6}$$

We treat the case of plane stress for which

$$\kappa = (5\lambda + 6\mu)/(3\lambda + 2\mu)$$

where λ and μ are Lamé constants of the beam material.
The stress boundary conditions are:

$$\begin{aligned} &\text{on } y = h,\ \sigma_{yy} = \tau_{xy} = 0 \\ &\text{on } y = 0,\ \tau_{xy} = 0;\ \sigma_{yy} = -p_1(x). \end{aligned} \tag{7}$$

The displacement boundary conditions depend on the end conditions of the beam.

2.1 *Simple supports*

To evaluate the transforms of derivatives of displacements (e.g. $u_{,xx}$) we shall use the following approximations in addition to the known boundary condition $v(\pm L, y) = 0$. First, we assume that

$$v_{,x}(\mp L, y) = \pm s$$

where s is the average slope of the beam at the supports due to load $p_1(x)$ obtained from classical beam theory. Actually, this has to be obtained as the difference in slopes due to load $p(x)$ and the U.D.L. $P/2L$. The other assumption on the boundary condition is that plane sections remain plane after bending. Thus,

$$u(\mp L, y) = \mp \left(y - \frac{h}{2}\right) s.$$

We also make use of the symmetry condition

$$u_{,x}(-L, y) = u_{,x}(L, y).$$

Physically, this means that the normal strains $\epsilon_{xx}(y)$ are the same on both the ends.

With the above conditions, eqns (6) transform as

$$-(\kappa+1)\xi^2\bar{u}+(\kappa-1)\bar{u}_{,yy}+2i\xi\bar{v}_{,y}=-(\kappa+1)i\xi\frac{s}{L}\left(y-\frac{h}{2}\right)\cos n\pi$$

$$-(\kappa-1)\xi^2\bar{v}+(\kappa+1)\bar{v}_{,yy}+2i\xi\bar{u}_{,y}=(\kappa-3)\frac{s}{L}\cos n\pi. \tag{8}$$

In the above equations $\bar{u}$ and $\bar{v}$ are functions of y and the transform variable n. The solutions of the above system of ordinary differential equations consist of complementary functions involving four arbitrary constants and particular integrals as given below.

$$\bar{v}(n, y)=(c_1+c_2y)\,e^{\xi y}+(c_3+c_4y)\,e^{-\xi y}-\frac{s}{\xi^2L}\cos n\pi \tag{9}$$

$$\bar{u}(n, y)=(d_1+d_2y)\,e^{\xi y}+(d_3+d_4y)\,e^{-\xi y}+\frac{is}{\xi L}\left(y-\frac{h}{2}\right)\cos n\pi \tag{10}$$

where

$$d_1=i\left(c_1+\frac{c_2\kappa}{\xi}\right)$$

$$d_2=ic_2$$

$$d_3=-i\left(c_3-\frac{c_4\kappa}{\xi}\right)$$

and

$$d_4=-ic_4.$$

c_1, c_2, c_3 and c_4 are functions of n and they are to be evaluated by using the stress boundary conditions (7). The stresses in (7) may be expressed in terms of displacements u and v. By taking transforms of these equations and substituting for $\bar{u}$ and $\bar{v}$ from eqns (9)–(10) we obtain the following set of simultaneous equations in unknowns $c_1 \ldots . c_4$.

$$\begin{bmatrix} 2\xi & (\kappa-1) & -2\xi & (\kappa-1) \\ 2\xi e^{\xi h} & e^{\xi h}\{(\kappa-1)+2\xi h\} & -2\xi\, e^{-\xi h} & e^{-\xi h}\{(\kappa-1)-2\xi h\} \\ 2\xi & (\kappa+1) & 2\xi & -(\kappa+1) \\ 2\xi\, e^{\xi h} & e^{\xi h}\{(\kappa+1)+2\xi h\} & 2\xi\, e^{-\xi h} & e^{-\xi h}\{2\xi h-(\kappa+1)\} \end{bmatrix} \begin{Bmatrix} c_1 \\ c_2 \\ c_3 \\ c_4 \end{Bmatrix} = \begin{Bmatrix} \frac{-\bar{p}_1}{\mu} \\ 0 \\ 0 \\ 0 \end{Bmatrix} \tag{11}$$

The above equations can be solved for c_1, c_2, c_3 and c_4 for any given n.

Substituting these values back in (9) and taking the inverse transform we obtain

$$v(x, y)=v_0(y)+\sum_{\substack{n=-\infty \\ n\neq 0}}^{+\infty}\bar{v}(n, y)\,e^{in\pi x/L}.$$

It can be shown that $\bar{v}(n, y)=\bar{v}(-n, y)$ and hence

$$v(x, y)=v_0(y)+2\sum_{n=1}^{\infty}\bar{v}(n, y)\cos(n\pi x/L). \tag{12}$$

The term $v_0(y)$ corresponds to $n=0$ and it cannot be evaluated from the general expression for $\bar{v}(n, y)$. So, the boundary condition $v(L, y)=0$ is used to evaluate $v_0(y)$. The displacements thus obtained are due only to $p_1(x)$. To obtain the final solution, the deflection due to the U.D.L. has to be added to the solution given in eqn (12).

2.2 *Clamped-clamped beam*

This can be considered as a special case with slope s at the ends being equal to zero.

2.3 *Numerical example*

As an illustration of the above developed method, the problem of a simply supported beam subjected to a constant load distribution over a portion of the length of the beam was solved. The v-displacements of points on the loaded surface are compared with beam solution. The results are given in Appendix A. The displacements obtained by the present method are slightly greater than the beam theory deflections. The maximum difference which is 0.16% occurs at the center of the beam. This may be because that part of the present solution is obtained from 2-D analysis which automatically takes the shear deformation into account. It has been found that at least one thousand terms have to be computed to get a good convergence of the solution given in (12). In general, convergence depends on contact length 2c. In the case of indentation problems, contact length will be very small compared to the length of the beam and more number of terms have to be taken into consideration for accurate evaluation of displacements and indentation. This may be explained by the fact that for smaller contact lengths, the load approaches Dirac delta function and higher harmonics decay very slowly.

3. INDENTATION BY A RIGID CYLINDER

Having developed a method for finding the displacements in a beam due to an arbitrary symmetric loading, we proceed to solve the problem of smooth indentation of a beam by a rigid circular cylindrical indenter of radius R and of unit length. The quantities of interest are contact length $2c$, contact stress distribution, total load, overall deflection of the beam, and the amount of indentation. We define the indentation as the difference in the vertical displacements of the indenter and the corresponding point on the bottom side of the beam.

We use two methods to compute the contact stresses: (i) method of point matching, (ii) assumed contact stress distribution. Once the contact stresses are found, other field quantities may be calculated by using the methods developed in Section 2.

3.1 *Method of point matching*

The contact length $2c$ is considered as known and the other quantities like stresses, deflection, etc. are calculated for a given contact length. The stress distribution under the indenter is asumed to be the superposition of a finite number of symmetrical rectangular loadings of unknown magnitudes distributed over known lengths (Fig. 2). For the sake of convenience, the contact length $2c$ may be divided into m equal parts as shown in Fig. 2. Thus,

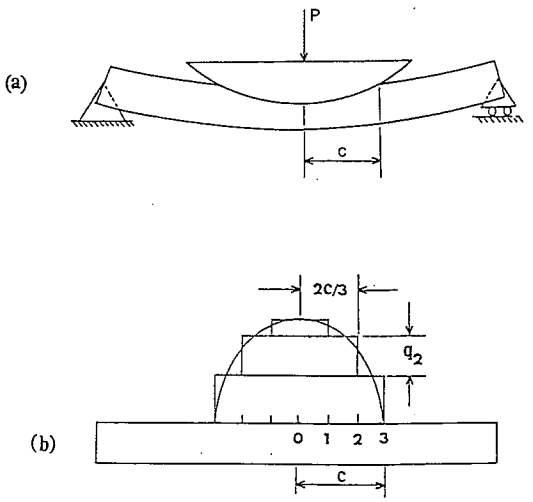

Fig. 2. (a) Cylinder indenting a beam. (b) Discretization of contact stress distribution.

the jth load distribution is of magnitude q_j and its span is $2cj/m$. To solve for the m unknown q's we need m equations which are set up by using the fact that the indented surface lies on a circular arc of radius R. To achieve this we consider m reference points on the contact surface excluding the center point. We also define the following: w_{jk} is the vertical displacement of jth reference point due to kth load distribution of unit magnitude; w_{ok} is the vertical displacement of the mid point of contact area due to kth load distribution of unit magnitude; v_j is the vertical displacement of jth point due to indentation; v_0 is the vertical displacement of the mid point due to indentation; and x_j is the x-coordinate of jth reference point.

From geometrical considerations, for contact lengths smaller in comparison with the radius of indenter we use the following approximate relation

$$(v_0 - v_j) \simeq x_j^2/2R \tag{13}$$

But

$$v_0 = \sum_{k=1}^{m} w_{0k} q_k \tag{14}$$

$$v_j = \sum_{k=1}^{m} w_{jk} q_k. \tag{15}$$

From eqns (13–15) we obtain

$$\sum_{k=1}^{m} (w_{0k} - w_{jk}) q_k = x_j^2/2R, \quad j = 1, \ldots, m. \tag{16}$$

The quantities w_{0k} and w_{jk} are like influence coefficients and they may be calculated using the methods described in Section 2. Thus we have m simultaneous equations (16) to solve for q's, the magnitudes of the rectangular load distributions over the contact area.

One can expect more accurate results as the number of divisions m increases. Once the contact stress distribution is obtained, vertical displacement of points $(0, 0)$ and $(0, h)$ may be computed. The total load is given by the summation of all rectangular loadings over the contact area. From the above quantities, beam compliance and indentation may be calculated. By varying the contact length $2c$, a whole series of load-indentation relations may be developed.

3.2 *Numerical examples*

The non dimensional stresses calculated using the above point matching technique are plotted in Figs. 3–5. They agree well with the results of Keer and Miller[1]. It may be seen that

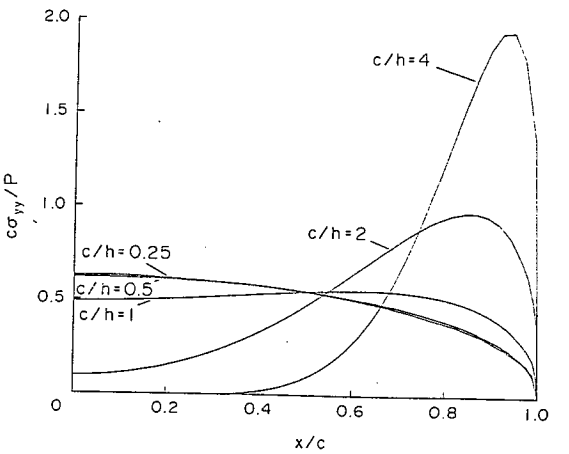

Fig. 3. Contact stresses for $L/h = 10$ and clamped ends.

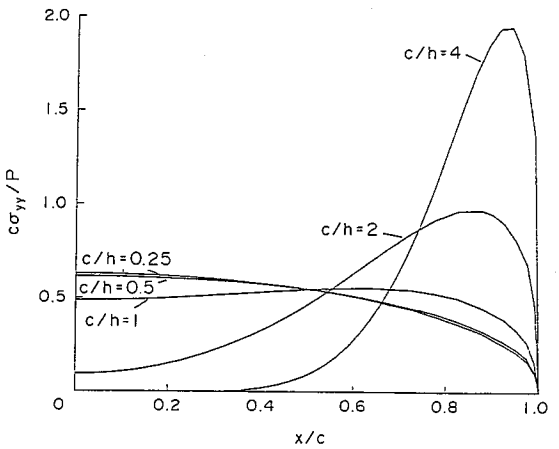

Fig. 4. Contact stresses for $L/h = 30$ and clamped ends.

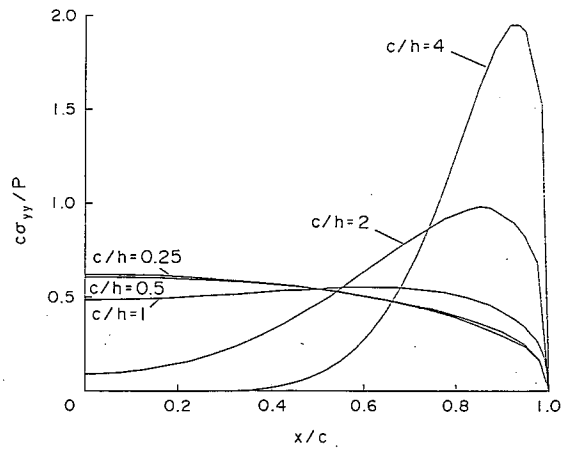

Fig. 5. Contact stresses for $L/h = 10$ and simple supports.

for smaller contact lengths ($c/h \leq 0.5$) the contact stress distribution may be represented by an ellipse as in Hertzian model. But for larger contact lengths there is an appreciable deviation from the Hertzian solution. For larger contact lengths, the stresses in the central portion of the contact region decreases and there is a peaking of stresses at the end zones. The same trend was also observed by Keer and Miller[1]. For $c/h \geq 3$, there is a region where contact stresses are zero. This is explained as follows: as the beam wraps around the cylindrical indenter, the radius of curvature of the beam becomes constant. This means that the bending moment has to be constant in the central portion, leading to zero shear force and zero normal stresses.

3.3 *Method of assumed stress distribution*

The fact that for small contact lengths the contact stress distribution approaches an ellipse may be used to solve the indentation problem in a more direct way. We assume a load distribution $p(x)$ over the contact length $2c$, given by

$$p(x) = p_0'(1 - x^2/c^2)^{1/2}$$

where p_0' is some arbitrary peak stress. Using the methods developed in Section 2 one can find the vertical displacements of the points in the contact zone. The average radius of curvature of

the indented surface R' may be calculated using the relation

$$R' = \frac{1}{m} \sum_{j=1}^{m} \frac{x_j^2}{2(v_0 - v_j)}$$

where m = number of reference points over the contact length; x_j = x-coordinate of jth reference point; v_0 = vertical displacement of the center point; and v_j = vertical displacement of the jth point. Generally, the value of R' is different from R, the radius of the indenter. But the displacements vary linearly with the load and hence the load p_0 required to produce a radius of curvature R is obtained from the relation

$$p_0 R = p_0' R'.$$

The desired load distribution is given by $p(x) = p_0(1 - x^2/c^2)^{1/2}$. Once p_0 is known, vertical displacements and indentation may be calculated as explained before.

In the numerical examples, numerical integration was used to evaluated the integral

$$\bar{p}(n) = \frac{1}{2L} \int_{-c}^{+c} p_0(1 - x^2/c^2)^{1/2} \cos \xi x \, dx.$$

4. RESULTS AND DISCUSSION

The numerical results presented in this section were obtained by using the point matching method for $c/h \geq 0.25$ and the assumed stress distribution method for $c/h \leq 0.25$. The Lamé constants λ and μ were assumed to be equal. This corresponds to a Poisson's ratio of 0.25.

Figure 6 and 7 depict the variation of contact area with the total load for small and large contact lengths respectively. From Fig. 6 it can be seen that the contact area increases rapidly at the beginning of indentation and thereafter varies almost linearly. Figure 7 shows that once again at higher loads there is a tendency for the contact length to increase by a larger amount even for a small increment of load. It is found that at this value of load, the radius of curvature of the beam approaches that of the indenter. Also this is the point where wrapping of the beam around the indenter begins.

The non-dimensionalized load-displacement curves are shown in Fig. 8. The initial portion of the curve is linear. At the point of beginning of wrapping, load-displacement relationship becomes non-linear and the beam becomes apparently stiffer. These results agree with [1].

In Fig. 9, beam compliances are plotted against contact length. The compliance values are normalized with respect to classical beam theory compliance C^* obtained by considering the

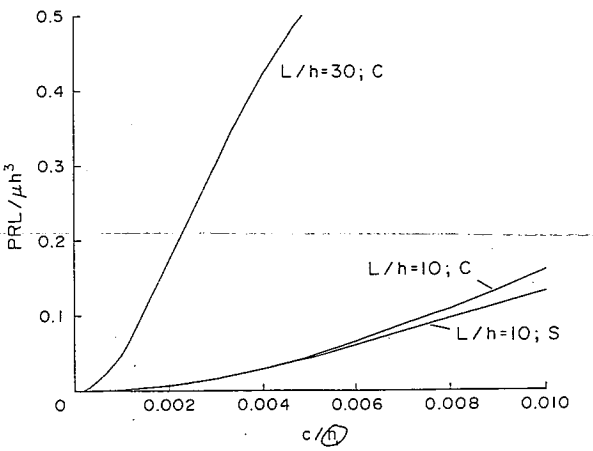

Fig. 6. Load-contact length relation for small contact lengths (C: clamped, S: simple supports).

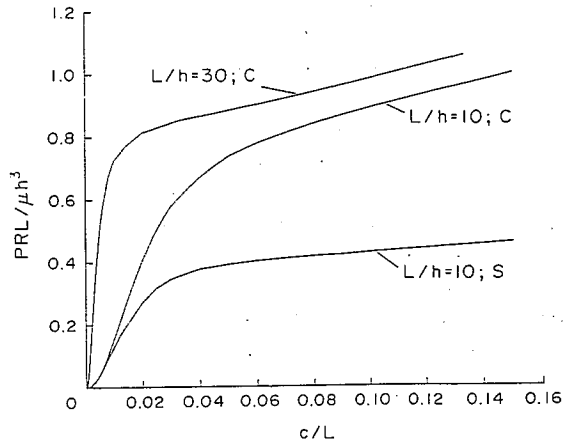

Fig. 7. Load-contact length relation for large contact lengths (C: clamped, S: simple supports).

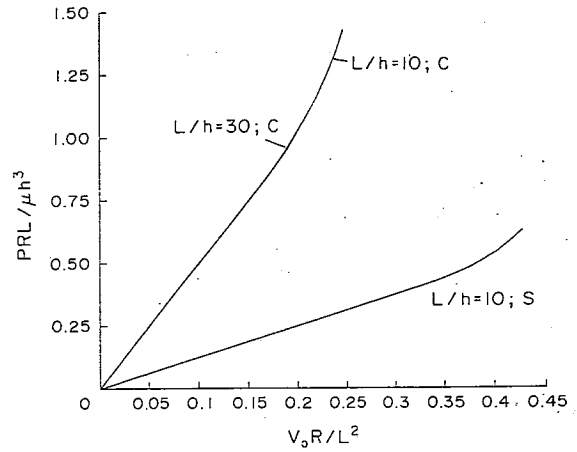

Fig. 8. Load-displacement relation (C: clamped, S: simple supports. Note: curves corresponding to $L/h = 10$; C and $L/h = 30$; C are indistinguishable.).

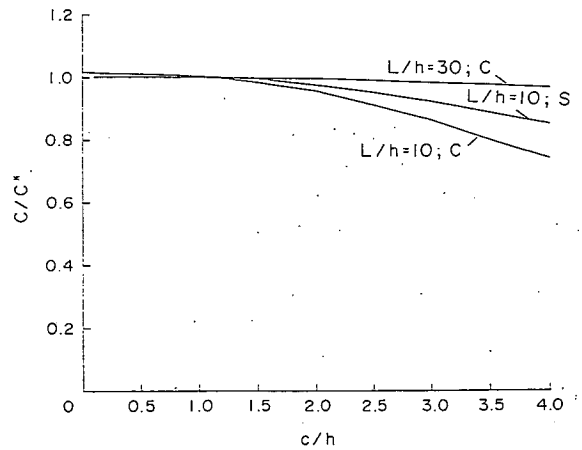

Fig. 9. Beam compliance versus contact length (C: clamped, S: simple supports).

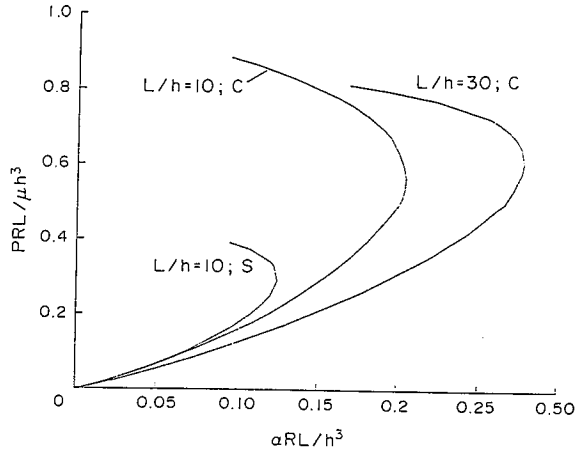

Fig. 10. Load-indentation relation (C: clamped, S: simple supports).

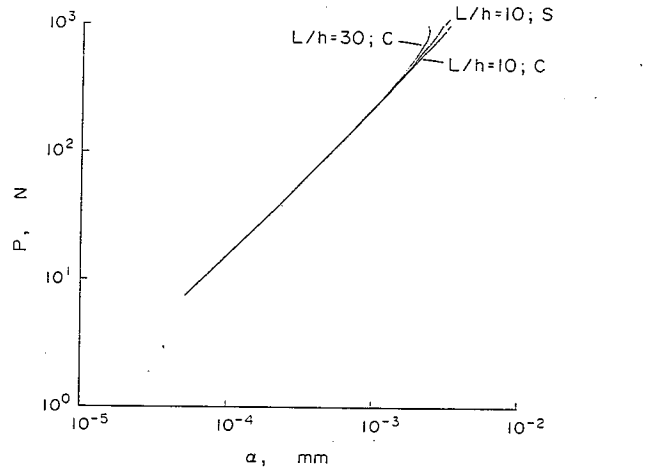

Fig. 11. Logarithmic plot of load-indentation relation (C: clamped, S: simple supports).

applied load as a point load. At the beginning of contact C/C^* is slightly more than unity. This is due to the fact that part of our solution is obtained from $2D$ analysis which automatically takes into account the shear deformation. As the contact area increases the beam appears to be stiffer. This is again due to the distribution of load over a finite area at higher contact lengths.

The load-indentation curves are shown in Figs. 10 and 11. In the beginning, indentation increases with the load and as will be shown later it can be modelled by a power law. As the load is increased further, at a point indentation becomes constant and starts decreasing with increasing loads. The explanation is as follows. According to our definition, indentation is the difference in displacements between the top and bottom points at the center of the beam. In the beginning the load is confined to a small contact area. This situation is close to a point load and so there is a significant difference in displacements of the top and bottom points of the beam at the center. But as the load increases, contact area also increases, distributing the load over a larger area. Such a distribution of load tends to reduce the difference in displacements and hence the indentation also starts decreasing.

Figure 11 is the logarithmic plot of load-indentation relationship. It may be noted that for small indentation, the contact law is the same irrespective of span and nature of end supports. It may also be seen that for small indentation, the load-indentation relationship can be modelled by a power law similar to the Hertzian contact law,

$$P = k\alpha^n.$$

A least squares fit of the data shown in Fig. 11 gave $n = 1.1254$. In general, k in the above formula is a function of radius of indenter and elastic constants of the beam material.

Acknowledgement—This work was supported by a NASA-Langley Research Center grant no. NAG 1222 with Purdue University.

REFERENCES

1. L. M. Keer and G. R. Miller, Smooth indentation of a finite layer. To appear in *ASCE J. Engng Mech. Div.*
2. H. D. Conway, S. M. Vogel, K. A. Farnham and S. So, Normal and shearing contact stresses in indented strips and slabs. *Int. J. Engng Sci.* **4**, 343, (1966).
3. C. T. Sun, An analytical method for evaluation of impact damage energy of laminated composites. *ASTM Special Publ. STP* 617, 427 (1976).

APPENDIX

The numerical example considered is a simply supported beam with load over a portion of its length. Length of the beam is assumed as 50.8 mm (2 in.). Thickness is 2.54 mm (0.1 in.) and width is taken as 25.4 mm (1 in.). A constant load of 0.1752 N/mm (11b/in) is applied over a length of 25.4 mm (1 in.). The load is assumed to be symmetrical about the center of the beam. Both the Lamé constants of the material are assumed to be equal to 6.8971 G Pa (10^6 psi). The vertical displacements of points on the loaded surface of the beam are computed using the method explained in Section 2. They are compared with the classical beam theory deflections in Table 1.

Table 1. Comparison of beam displacements computed with the present method and the classical beam theory

	Vertical Displacements (x 10^{-3} mm)		
x/L	Present Method	Classical Beam Theory	% Difference
0.1	17.898	17.869	0.16
0.2	17.218	17.191	0.16
0.3	16.105	16.081	0.15
0.4	14.590	14.570	0.14
0.5	12.714	12.700	0.11
0.6	10.534	10.526	0.076
0.7	8.1117	8.1077	0.049
0.8	5.5077	5.5067	0.018
0.9	2.7828	2.7838	-0.036
1.0	0.0	0.0	0.0